The Electrical Characteristics of Human Skin *in Vivo*

Yogeshvar N. Kalia[1] and Richard H. Guy[1,2]

Received January 31, 1995; accepted June 27, 1995

Purpose. The objectives of this study were to investigate the impedance properties of human skin *in vivo* and to examine the effect of iontophoresis upon them.

Methods. Having established the intra- and inter-individual variation in basal values of skin impedance, the effect of varying iontophoretic current density, ionic strength and counter-ion on the rate of recovery of skin impedance after iontophoresis was investigated.

Results. Passage of an iontophoretic current caused a significant reduction in the magnitude of the skin impedance. Increasing the current density caused an even greater reduction in the value of the skin impedance and slowed the rate of recovery. Reduction of the ionic strength resulted in an increase in the rate of recovery following iontophoresis. A significant increase in the rate of recovery was observed when $CaCl_2$ replaced NaCl as the electrolyte. Although visual inspection revealed the presence of greater erythema when $CaCl_2$ was used, there was an absence of the mild sensation experienced by volunteers when using NaCl. The last part of the study established a correlation between transepidermal water loss and impedance analysis as complementary methods for probing skin barrier function *in vivo*. The data were fitted to an equivalent circuit consisting of a resistor in parallel with a constant-phase element and a mechanistic model proposed to explain the electrical properties of the skin.

Conclusions. The first comprehensive investigation of the effect of iontophoresis on the electrical properties of human skin *in vivo* has been described. It would appear from the results, and from their interpretation, that impedance spectroscopy may be an effective method to quantify the impact of iontophoresis on the skin, and to determine the extent to which proposed drug delivery regimens will perturb skin barrier function.

KEY WORDS: impedance spectroscopy; human skin *in vivo;* iontophoresis; transdermal drug delivery.

INTRODUCTION

The efficacy of the skin as a defensive barrier (1) has a less desirable corollary–the transport of beneficial therapeutic agents is also reduced. Iontophoresis provides a powerful, controllable method for the enhanced delivery of molecules through the skin (2). In this study, we have monitored the electrical impedance characteristics of human skin *in vivo* and investigated the changes induced by iontophoresis. In our view, *in vivo* measurements must be made in order to develop effective methods that can cope with intra- and inter-individual variability since the controlled delivery of a therapeutic agent must be modulated to respond to changes in skin permeability at the delivery site at the time of drug delivery.

In a previous study, Yamamoto and Yamamoto measured the impedance properties of human skin *in vivo*. Specifically, they studied the variation of skin impedance as the stratum corneum was progressively tape-stripped (3). Removal of the stratum corneum was shown to drastically reduce the value of the observed electrical resistance which, in turn, led to the deduction that the intrinsic resistance resides in this layer of the skin. The lipid milieu is suggested as being the source of the reactive (essentially capacitive) contribution. The classical equivalent circuit model for the stratum corneum employs a parallel arrangement of a resistor and a capacitor. The principal drawback of such a model is that it predicts an impedance locus having a semi-circular arc with its origin located on the resistance (real) axis. This is not observed experimentally: the impedance locus has an origin that lies *below* the resistance axis (by convention, the negative reactance (imaginary) axis is plotted along the positive ordinate axis). Refinement of the parallel RC circuit model was necessary to explain the effect of enhancers on human stratum corneum *in vitro* (4). Kontturi *et al.* (4), and Kontturi and Murtomäki (5), introduced a constant-phase element (CPE) into their three-branch equivalent circuits to explain the effects of permeation enhancers on human cadaver skin. This circuit element gives rise to an impedance locus having a depressed center.

The first stage of our investigation addressed the issue of intra-individual variation in skin impedance as a function of time, leading to the question, what is the underlying inter-individual fluctuation of skin impedance *in vivo* observed on a day-to-day basis? The effect on skin impedance as the distance between the electrode chambers on the subject's forearm increased was also studied. The impact of hydration on skin impedance was investigated by making repeated impedance measurements at the same site. The ultimate aim of these control measurements was to permit the changes in skin impedance due to iontophoresis to be distinguished from those caused by hydration of the stratum corneum. Having established the intra-individual variability, the second phase of the work examined how skin impedance was affected by passage of an iontophoretic current. Impedance spectra were recorded under passive (pre-iontophoresis) conditions and in the post-iontophoretic state to investigate the effect of iontophoresis upon the electrical properties of the skin *in vivo*.[3] The next phase of the study focused on how increasing iontophoretic current density affected skin impedance. The role of ionic strength was also investigated. In addition, the effect of the counter-ion on the recovery process was examined. The third part of the study dealt with the question: can impedance spectroscopy be used as an accurate measure of skin permeability? Impedance data were correlated with transepidermal water loss (TEWL) measurements. Whereas TEWL directly measures the rate of water

[1] Departments of Pharmacy and Pharmaceutical Chemistry, University of California at San Francisco, San Francisco, California 94143-0446.

[2] To whom correspondence should be addressed.

[3] Preliminary measurements of this type have been reported: S. Y. Oh & R. H. Guy, "Effects of iontophoresis on the electrical properties of human skin *in vivo*", Internat. J. Pharmaceut., **124**:137–142 (1995).

0724-8741/95/1100-1605$07.50/0

loss across the skin, impedance measurements offer mechanistic insight into the passage of charged and polar species in general. The permeability of skin to a charged molecule is intimately related to the degree of hydration since water provides the most favorable environment for an ionic species; in other words, it offers a low impedance pathway for ion transport. Finally, a simple equivalent circuit model, consisting of a parallel R-CPE circuit, that was capable both of fitting the experimental data and of providing a physically meaningful interpretation of the results was developed. Following Occam's Razor, we used a model that retains the simplicity and ease of interpretation of the RC-circuit, but which provides a more accurate fit to the experimental data.

MATERIALS AND METHODS

Chemicals. N-2-hydroxyethylpiperazine-N'-2-ethanesulphonic acid (HEPES) buffer and NaCl were obtained from Sigma Chemical Company (St. Louis, Missouri). $CaCl_2$ was from Fisher Scientific (Fair Lawn, New Jersey). Deionized water (resistivity $\geq 18M\Omega\ cm^{-1}$) purified by a Millipore System (Milli-Q UFplus), was used to prepare all solutions.

Electrodes. All electrodes were Ag/AgCl electrodes prepared by chloridizing silver wire (1mm diameter, 99·99% pure; Aldrich Chemical Company,) immersed in 133 mM NaCl solution (Pt-cathode) for approximately 3 hours at an applied current of 0·5mA.

Experimental Apparatus. A Macintosh Quadra 800 (Apple Computers Inc., Cupertino, California) equipped with LabVIEW 3.0.1 (National Instruments Inc., Austin, Texas) was used to control a HP8116A Pulse/Function Generator (Hewlett-Packard Co., North Hollywood, California). At an applied voltage of 1·0V (peak-to-peak), this produced a sinusoidal alternating current whose frequency was raised from 1Hz to 1·6kHz incrementally with 8 frequency points sampled per decade. The electrical circuit used for making the impedance measurements included a 2MΩ resistor in series with the skin. Thus, at the applied voltage of 1·0V (peak-to-peak), the sinusoidal current remained approximately constant (≈0·25μA). The potential difference across the skin was measured using a Stanford Research Systems SR850 DSP Lock-In Amplifier (Stanford Research Instruments Inc., Sunnyvale, California). An isolation transformer (Professional Design and Development Services, Berkeley, California) protected the human subject by ensuring complete isolation of the volunteer from the main power supply. TEWL measurements were made using a Servo Med Evaporimeter EP1 (Servomed AB, Stockholm, Sweden). All data were analyzed using the Microsoft Excel (version 4.0 Copyright © 1985-1992) software package.

Experiments

1. Intra-Individual Variation in Skin Impedance. Two electrode chambers were attached securely to the individual's ventral forearm with adhesive tape (3M, St. Paul, Minnesota). The chambers contained 5ml of 133mM NaCl and 25mM HEPES at pH 7·4. The chambers were placed 3·0-5·0cm apart. Each chamber contained two electrodes—one for applying the signal, the other for sensing. The exposed area of the skin in each chamber was $3·14cm^2$. An impedance spectrum was recorded; then one of the cells was moved to increase the separation between the two electrode chambers to ~9cm. A second impedance spectrum was recorded. Subsequently, a third impedance spectrum was recorded with the separation further increased to 12·0-14·0cm.

This procedure was repeated over a period of three days to establish the variation of the basal impedance for that subject.

2. The Effect of Hydration on Skin Impedance. To investigate whether hydration had a significant effect on the local impedance, the electrode chambers were set up as described above and an impedance spectrum recorded immediately. Three more spectra were subsequently recorded without changing the position of the electrode chambers, over the next 30 minutes. As a control experiment, electrode chambers filled with buffer were secured to the other arm and the skin allowed to hydrate for a period corresponding to the time taken for acquisition of a complete impedance spectrum before beginning data acquisition.

3. Inter-individual Variation in Skin Impedance and the Effect of Iontophoretic Current Flow. The electrode separation was held constant at approximately 6·0-7·0cm. An initial impedance spectrum was recorded to obtain the passive impedance level of the subject. The skin was only partially hydrated at the beginning of the experiment. Then, an iontophoretic current (delivered using a Kepco Power Supply APH 100M, Flushing, NY) of $0·1mA\ cm^{-2}$, was applied for 15 minutes. The first post-iontophoresis impedance spectrum was recorded immediately upon termination of the iontophoretic current flow. Another impedance spectrum was recorded 30 minutes later to assess the rate of recovery of skin impedance.

4. Effect of Varying the Iontophoretic Current Density. The above experiment was repeated with the current density increased to $0·2mA\ cm^{-2}$.

5. Effect of Ionic Strength on Skin Impedance. The ionic strength of the electrode solutions was decreased 10-fold; (i.e., the buffer consisted of 13·3mM NaCl and 2·5mM HEPES), and the procedure described in section 3 repeated. To minimize the effect of day-to-day intra-individual variation in impedance observed over 24 hours, experiments with the standard and diluted buffer concentrations were carried out consecutively on the subject on the same day using corresponding sites on left and right forearms.

6. Effect of the Counter-Ion on Skin Impedance. An experiment as described in section 3 was performed on the subject's left arm using NaCl as the electrolyte. Then, the same experiment was performed on the subject's right arm, but with NaCl replaced by the same concentration of $CaCl_2$. Three impedance spectra were recorded: the first measurement was made prior to iontophoresis; the second and third measurements were made immediately after iontophoretic current flow, and then 30 minutes later, respectively.

7. Correlation Between Skin Impedance and TEWL Measurements. TEWL measurements were made on both forearms. Then, the electrode chambers were placed (~6 cm apart) on the subject's right forearm and an impedance spectrum recorded. The left arm was then subjected to repeated tape-stripping using Scotch No. 845 Book Tape (3M St. Paul, MN); between 20 and 30 tape-strips were removed. A TEWL measurement was made after every second tape-

strip. Once the tape-stripping procedure was complete, an impedance spectrum was recorded on the tape-stripped skin.

RESULTS

The intra-individual variation in impedance is illustrated in Figure 1a. The impedance spectra were basically semi-circular in shape, although the center lay below the real-axis. At low frequencies ≤100 Hz (lowest sampling frequency = 1Hz, low frequency data points are located at the right hand side of the figure), the impedance loci did not curve significantly towards the real-axis. Electrode separation did not have a major effect on the impedance loci. This is because the primary barrier to current flow is the stratum corneum; current flow is more facile in the underlying aqueous tissue layers. Our data confirm the wide range in the "basal" level of *in vivo* skin impedance and underline the importance of performing *in vivo* studies to evaluate variation in skin impedance and its implications for transdermal drug delivery (data from all subjects not shown). Inada *et al* found the resistance of excised human epidermal tissue to lie in the range (12-120 kΩ cm^{-2}) (6). These values are, on the whole, lower than those found for the majority of subjects which we have studied, although the upper limit begins to overlap the values found in our study. Note that, because of our experimental arrangement, the observed impedance represents twice that of the stratum corneum.

The effect of hydration on skin impedance is shown in Figure 1b. The first impedance locus was similar to those shown in Figure 1a. However, the remaining spectra did exhibit curvature towards the real axis at low frequency and indicated much lower impedance values: in the first spectrum, the real component of the impedance, Z_{Real} was 187kΩ at 1Hz whereas for the second spectrum, Z_{Real} had decreased to 82kΩ. The control experiment, in which the electrode chambers containing buffer were left in contact with the skin for a period of 15 minutes (approximately equal to the duration of an impedance sweep), produced a spectrum showing a comparable reduction in impedance values (Figure 1b).

The impedance spectra from a subject before and after application of an iontophoretic current of 0·1mA cm^{-2} for 15 minutes are shown in Figure 2. The preiontophoresis impedance spectrum was recorded, without allowing for hydration of the skin, and exhibited a circular arc, although, as described above, the center of the impedance locus lay below the real axis. The second impedance spectrum was recorded immediately after passage of an iontophoretic current. These impedance loci possessed a completely different geometry. At the low frequency end of the spectrum, the loci coiled back upon themselves. This may have been due to the measurement having been made while the system was in a dynamic state, as it searched for a new equilibrium once the iontophoretic current had been removed. The third spectrum was recorded 30 minutes after cessation of the iontophoretic current. In contrast to the second spectrum, the third again showed essentially circular behavior with a depressed center. There were distinct inter-individual differences in response to the application of an iontophoretic current.

A comparison of the impedance data obtained after application of 0·1mA cm^{-2} and 0·2mA cm^{-2} (Figure 3a) showed the significantly more pronounced effect upon skin impedance of the larger iontophoretic current. Although the pre-iontophoresis spectra failed to show any significant variation, the post-iontophoretic spectra recorded using the higher ionic strength buffer (Figure 3b) displayed much lower impedances (note the tighter impedance loci). In addition, the spectra indicated that higher ionic strength led to a slower rate of recovery of basal impedance levels. The experiments comparing the effect of sodium and calcium on the rate of recovery produced intriguing results (Figure 3c). Although the spectra obtained immediately after termination of the iontophoretic current showed comparable impedance values—with the spectrum obtained using $CaCl_2$ as the elec-

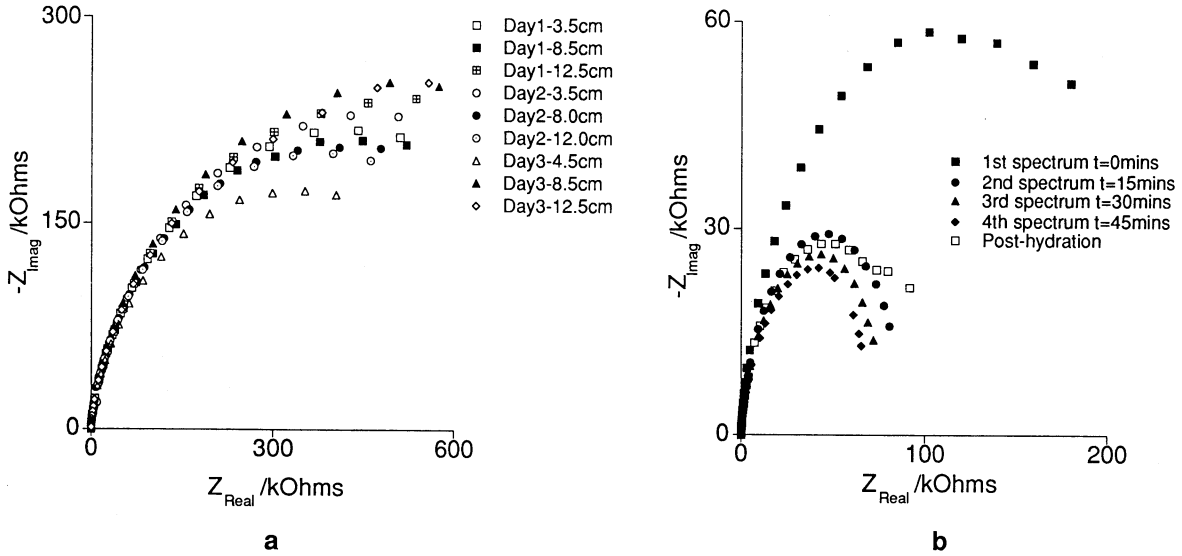

Fig. 1. (a) Intra-individual variation of impedance as a function of time and electrode separation. The impedances shown in this figure and in all subsequent figures, are given per unit area. Data from subject B. (b) The complex plane impedance spectra obtained after repeated measurements at the same site on a subject's forearm. Data from subject E.

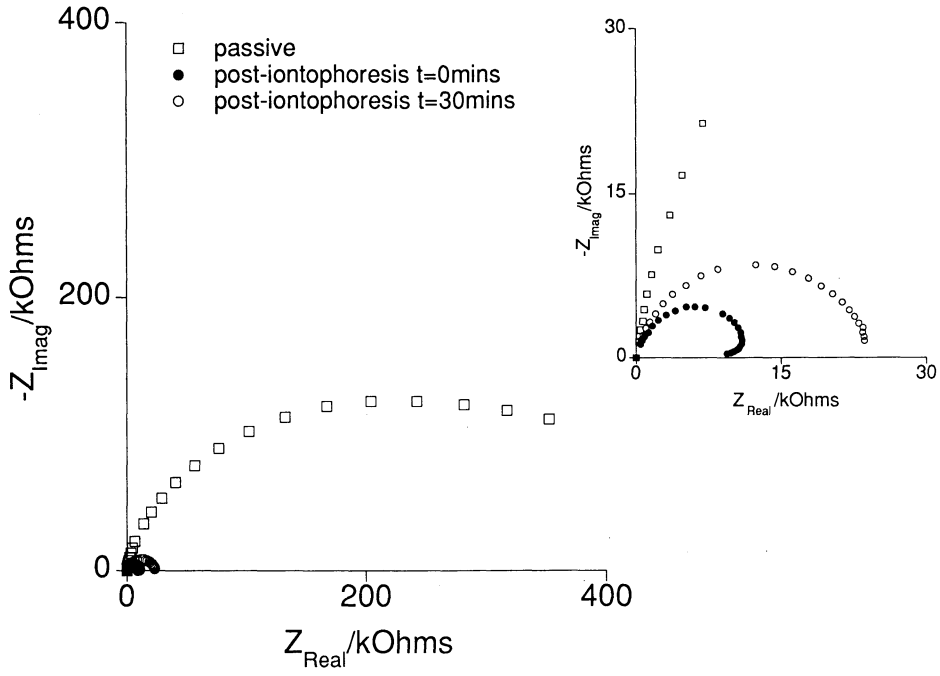

Fig. 2. Complex plane impedance spectra before and subsequent to application of an iontophoretic current of 0·1mA cm^{-2} for 15 minutes. Data from subject B.

trolyte showing a slightly lower impedance—the second pair of spectra recorded 30 minutes after iontophoresis were markedly different. There was significantly greater recovery of basal impedance using $CaCl_2$. Moreover, the subjects felt no sensation during iontophoresis in the presence of calcium ions, in contrast to the "tingling" sensation that was experienced by all subjects with NaCl. Surprisingly, visual inspection of the skin below the anode chamber showed greater erythema when $CaCl_2$ was used. That is, greater erythema did not coincide with a higher degree of discomfort. It is also noted that, despite the fact that increased ionic strength retarded the rate of recovery of skin impedance (although identical concentrations of NaCl and $CaCl_2$ were used, the ionic strength of the latter solution was obviously greater), the use of $CaCl_2$ still increased the recovery rate. Burnette has proposed that Ca^{2+} may have greater difficulty crossing the stratum corneum owing to a greater binding affinity with skin's negatively charged sites (7). This would reduce the free ion content in the stratum corneum and would counteract the expected enhanced transport owing to the increase in charge.

The correlation between electrical impedance data and transepidermal water loss (TEWL) measurements is shown in Figure 4. The TEWL data showed a clear increase as the stratum corneum was removed by sequential tape-stripping. Concurrently, the impedance decreased since the stratum corneum is the tissue responsible for preventing the flow of current.[4] The decrease in skin impedance, although significant, was smaller than that described by Yamamoto and Yamamoto (3) because we did not tape-strip away all the stratum corneum. Subsequently, when we did continue tape-stripping until the skin surface glistened, suggesting complete removal of the stratum corneum, skin impedance values agreed with the earlier findings (3) (unpublished results).

DISCUSSION

The central theme of this work is to characterize the effect of iontophoresis on the electrical impedance characteristics of human skin *in vivo*. It then becomes possible to address our long-range goal—optimization of the conditions that facilitate iontophoretic enhancement of transdermal drug delivery. The basic parallel RC-circuit model for a biological membrane has an impedance given by

$$Z_m = \frac{R_m}{1 + j\omega C_m R_m} \quad (1)$$

where Z_m = membrane impedance (Ω), R_m = membrane resistance (Ω), C_m = membrane capacitance (F), and ω = angular frequency (rad s^{-1}).

A more accurate representation replaces the capacitor with a constant-phase element (CPE). A CPE can be considered as having a phase-angle of $\alpha\pi/2$, where α is a frequency-independent constant that determines the distance below the real-axis of the center of the impedance locus. It has an impedance of the form, $1 / A(j\omega)^{\alpha}$, where A is a constant. When $\alpha = 1$, the CPE behaves as an ideal capacitor, when $\alpha = 0$, it behaves as a pure resistor. The impedance of a parallel R-CPE circuit is given by,

$$Z_m = \frac{R_m}{1 + (j\omega)^{\alpha} A R_m} \quad (2)$$

[4] Y. N. Kalia, L. B. Nonato and R. H. Guy, "Correlation between impedance spectroscopy and transepidermal water loss: non-invasive probes of human skin permeability *in vivo*", Conference Proceedings: Prediction of Percutaneous Penetration: Methods, Measurements & Modeling, Fourth International Conference 19-22 April (1995), in press.

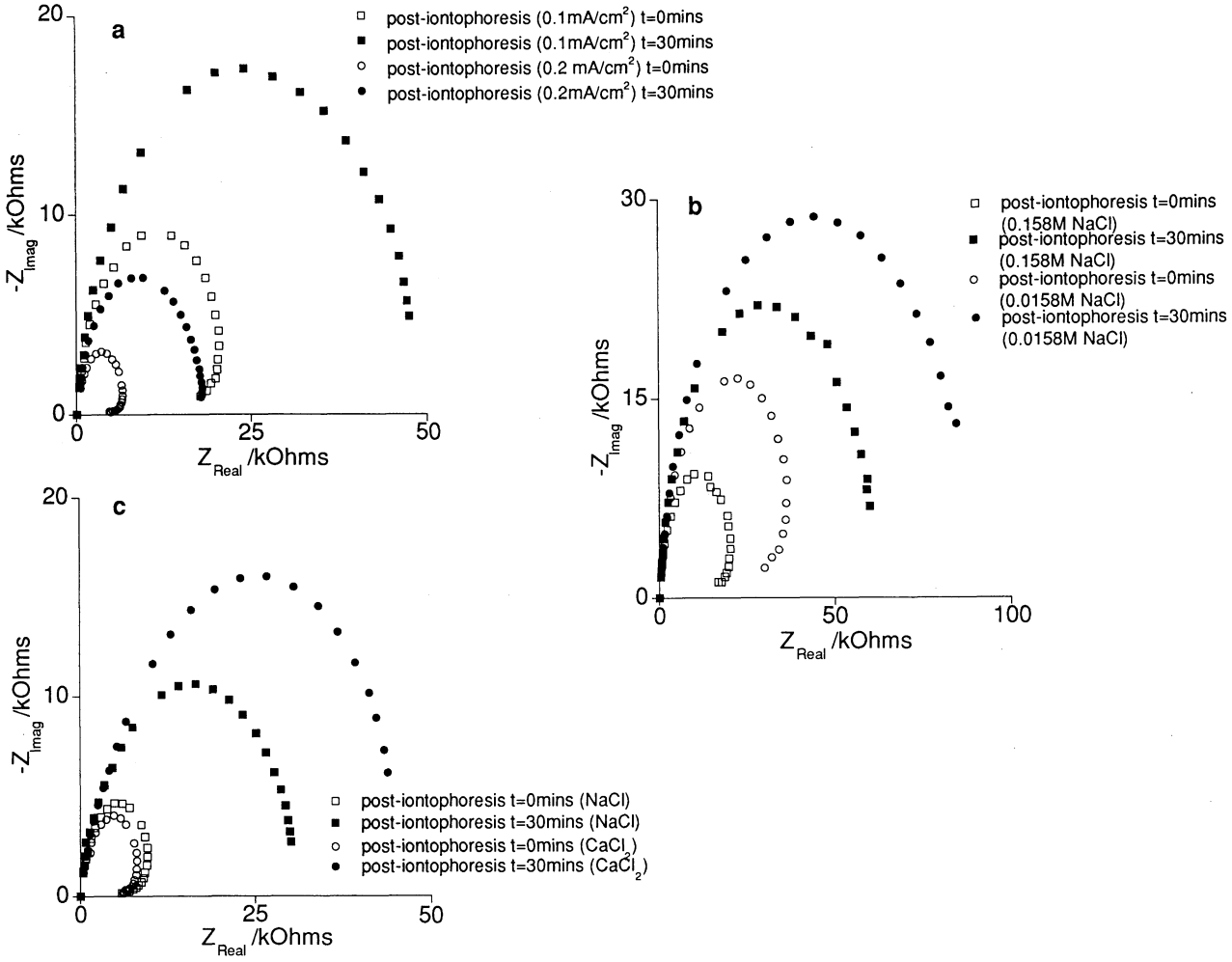

Fig. 3. (a) Complex plane impedance spectra showing the effect of increasing the iontophoretic current density. Data from subject C. (b) Complex plan impedance spectra post-iontophoresis as a function of the ionic strength of the electrolyte. Data from subject F. (c) Complex plane impedance spectra showing the differences observed when using 0.154 M NaCl or 0.154 M $CaCl_2$ as the electrolyte. Data from subject D. The current density for the experiments shown in (b) and (c) was 0.1 mA cm^{-2}.

The center of the locus in the complex plane impedance plot for a parallel R-CPE circuit is characteristically depressed, as observed for skin. Equivalent circuits utilizing CPEs have been used previously to model biological membranes, for example, the red blood cell membrane (8).

Kontturi *et al.* (4) defined the constant, A (which is denoted by Y in their manuscript), as the admittance of the CPE; however, A is more accurately a constant whose dimensions depend on the value of α, and hence on the nature of the admittance of the CPE. For example, when $\alpha = 1$, A represents the capacitance, C.

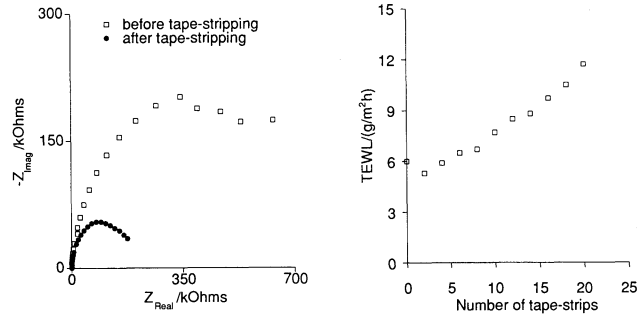

Fig. 4. Correlation between impedance measurements and TEWL. Data from subject D.

Since graphical fitting techniques cannot be used to determine accurately the electrical parameters for an R-CPE circuit, we have used complex nonlinear least squares (CNLS) data fitting (9) to obtain equivalent circuit system parameters. In contrast to the three-branch circuits used by Kontturi and coworkers (4,5), we have fitted the data to a simple, parallel R-CPE circuit (as described by equation 2) using the CNLS immitance fitting program LEVM (version 6.1) (10). The experimental data and the corresponding CNLS fits are shown in Figure 5 and Table I. The pre-iontophoresis impedance spectrum produced before the skin becomes fully hydrated is difficult to fit using either the R-CPE parallel circuit or the 4-component R-CPE model (7) (Figure 5a). The system is in a dynamic state and the observed locus may be a composite of a series of loci; in other words, successive data points lie on different parent loci

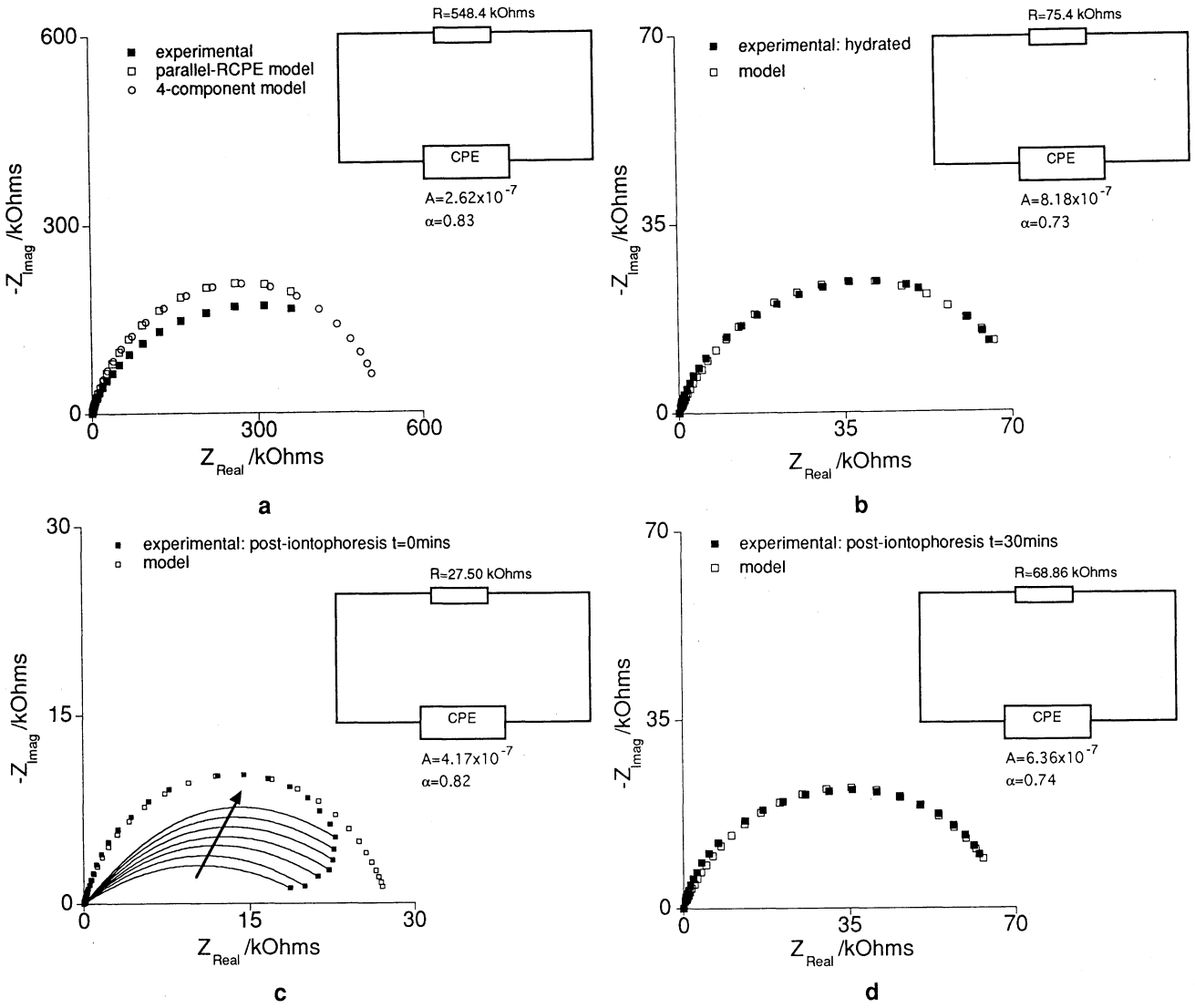

Fig. 5. (a) Comparison of the experimental impedance locus obtained prehydration with the CNLS fits predicted by the parallel R-CPE model and the 4-component CPE-containing circuit (7). Data from subject B. (b) The impedance spectrum produced after hydrating the skin for 45 minutes and the CNLS fit produced using the R-CPE parallel circuit. Data from subject E. (c) The first impedance locus produced after passage of an iontophoretic current and the corresponding CNLS fit generated by the R-CPE model. The accuracy of the fit decreases with decreasing frequency. Since the spectrum is recorded immediately after termination of the applied iontophoretic current, the system is in a state of flux as the ions present attain new equilibrium concentrations. The solid lines suggest what might be observed if instantaneous sampling over the complete frequency range were possible. During the course of the frequency sweep, the system "hops" from one curve to the next outer curve as it seeks a new stable state. The arrow indicates increasing time during the experiment. Data from subject B. (d) The second post-iontophoresis impedance spectrum recorded 30 minutes after iontophoresis and the corresponding CNLS fit predicted by the R-CPE model. Data from subject B.

which reflect the progressive decrease in skin impedance as the system gradually attains a new equilibrium during the time-course of the experiment. Thus, designing an equivalent circuit to accurately fit the data would require one to model a time-varying system. The impedance locus of hydrated skin is modeled accurately by the parallel R-CPE equivalent circuit (Figure 5b). The skin impedance is dominated in the low frequency region by the reactive (capacitive) element; thus, charge passes along resistive shunt pathways. As the frequency is increased, the impedance due to the reactive (capacitive) component decreases until, at higher frequencies, it provides negligible opposition to the flow of charge. Note that the experimental data are fit with α = 0·73; whereas, for an ideal capacitor, α = 1. This difference highlights the inability of the simple parallel RC-circuit to provide an accurate model for the skin.

The impedance spectrum produced immediately after termination of iontophoretic current flow is complex. The ions no longer experience a driving force and must establish a new equilibrium state (Figure 5c). The poor fit at low frequency is due to the inability of the circuit to cope with the dynamic nature of the system as it seeks a new equilibrium. It is also possible that the impedance is influenced by the reversal of any potential-induced structural changes that fa-

Table I. Representative Equivalent Circuit Parameters (Mean ± Error) for the Parallel R-CPE Circuit (see Figure 5) Used to Model the Impedance Behavior of Human Skin *in vivo*

Skin state[a]	Equivalent circuit parameters		
	R[b]	A[c]	α[d]
Passive[e] (before hydration)	548.4 ± 3.6[g] kΩ	(2.62 ± 0.02) × 10^{-7}	0.83 ± 0.002
Hydrated[f]	75.41 ± 0.35 kΩ	(8.18 ± 0.13) × 10^{-7}	0.73 ± 0.004
Post-iontophoresis t = 0 minutes[e]	27.50 ± 0.31 kΩ	(4.17 ± 0.22) × 10^{-7}	0.82 ± 0.010
Post-iontophoresis t = 30 minutes[e]	68.86 ± 0.31 kΩ	(6.36 ± 0.12) × 10^{-7}	0.74 ± 0.004

[a] Circuit parameters are given for impedance data collected both prior to and after iontophoresis. In addition, data have been fitted for hydrated skin.
[b] Value of resistance in parallel R-CPE circuit. Values are per unit area (cm^2).
[c] Value of admittance-related constant of the CPE.
[d] Value of the constant determining the phase-angle of the CPE.
[e] Data from Subject B.
[f] Data from Subject E.
[g] Errors indicate the goodness of fit of the model to the experimental data.

cilitated transport. A similar situation to that for the primarily unhydrated state exists, namely, the early data points may originate from different impedance loci, each point representing a "snap-shot" of the impedance at that frequency, but successive points belonging to different parent loci. During the course of the experiment, the system "hops" from one curve to the next and the experimental measurements are sampled from a set of loci (Figure 5c). This would explain the curvature of the locus in the low frequency region. As the frequency is increased, with increasing time after termination of the iontophoretic current, the quality of the CNLS fit improves as the equilibrium is reached. For this case, R has been further reduced, to 27·5kΩ and α = 0·82. To test the hypothesis that the unusual geometry shown in the first post-iontophoresis spectrum was caused by relaxation processes occurring while the measurement was being made, the frequency sweep was started at the upper frequency limit and decreased to 1Hz (Figure 6). The data then exhibit the more typical geometry, suggesting that the system had essentially reached a new equilibrium state by the time that the low frequency measurements were made. The second post-iontophoresis spectrum is modeled very successfully by the R-CPE circuit confirming that the system is now in a stable state (Figure 5d). The quality of the fit is uniformly high across the frequency range. The value of α has fallen to 0·74, from the high of 0·82 immediately after application of an iontophoretic current. This value is very close to that observed for hydrated skin (α = 0·73). The value of the parallel resistance, R, has increased to 68·9 kΩ.

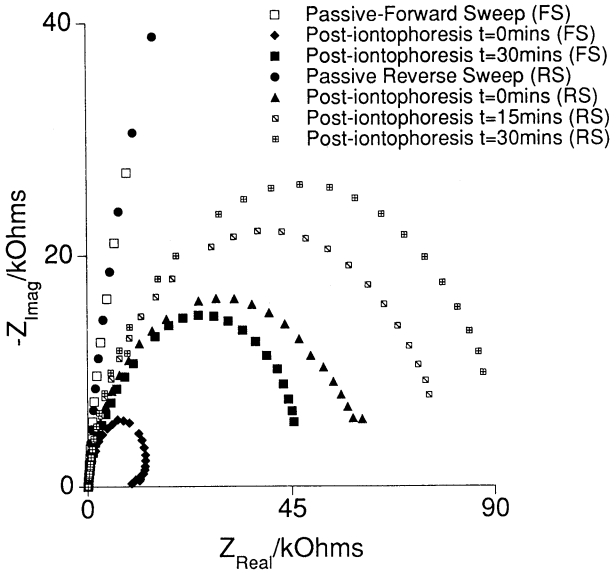

Fig. 6. The post-iontophoresis spectra obtained when the frequency sweep was begun at the upper frequency limit. The "forward sweep" spectra are shown for comparison. Data from subject D.

The *in vivo* data are consistent with the kinetic model of Keister and Kasting who proposed that the rate of transport is limited by the presence of potential-dependent energy barriers (11). This model describes the loss of skin resistance as the result of reorientation of molecules along the ion transport pathway under the influence of the applied current. Since appendageal pathways are considered to be the sites of highest current density (12,13), lipid molecules present in the hair follicles and the sweat glands have been suggested to undergo realignment with the applied electrical field.

The initial, passive spectrum reflects, primarily, the impedance properties of unhydrated skin, which has a high impedance. As the degree of hydration increases, the impedance falls as the local ion concentrations increase and the skin becomes loaded with additional charge-carriers. Application of an iontophoretic current causes the impedance to decrease sharply. The applied field can induce conformational changes in the lipid/protein molecules, forcing them to adopt high energy conformations that facilitate charged ion transport, thereby enlarging pre-existing channels. Alternatively, the decrease in the impedance may be due to the reorientation of lipids or keratin bundles in the bulk stratum corneum and the formation of transient conduction channels. In addition, the ion concentration in the resistive pathways may rise sharply, increasing the number of charge carriers and thus reducing the impedance. However, once the external field is removed, the system begins to relax and the majority of the current-induced transient pathways begin to disappear. The changing ion concentrations, or perhaps, the

relaxation of potential-induced structural effects in this dynamic state (e.g., the iontophoretically induced enlargement of existing transport channels) can explain the unusual geometry observed in the first post-iontophoretic impedance locus. The initial region of the impedance spectrum may be an ensemble of a series of impedance spectra with successive data points originating from different spectra which reflect the state of the system. As the time following current passage increases, the skin produces spectra, exhibiting higher impedance values, similar to those for the pre-iontophoretic, hydrated state.

The heterogeneity of skin implies that, when a voltage is applied, the current flows non-uniformly. The resistor, R, in the parallel R-CPE circuit can be viewed as ionic conduction channels whose resistance falls as the number of charge carriers increase or as potential-induced structural changes occur. The first decrease is caused by the hydration of the skin and a second, more dramatic reduction, is caused by iontophoresis. However, in addition to these purely resistive pathways, there can exist reactive, capacitor-like, regions. These may be lipid- or protein-rich domains that can be considered as a dielectric medium in a capacitor. As the charge builds up on one side of the dielectric, a potential difference is created, and the changing frequency of the sinusoidal potential causes a reactive (capacitive) current to be generated on the other side. Thus, charge does not flow directly across these regions but reactive (capacitive) currents are produced that are proportional to the rate of change of the potential difference. The impedance of the skin is inversely proportional to the the current (I_m) flowing through it, i.e. (14),

$$I_m = C_m \frac{\partial V_m}{\partial t} + \frac{V_m}{R_m} \qquad (3)$$

where V_m = potential difference across the skin (V). The increasing frequency of the applied sinusoidal potential difference causes $\partial V_m/\partial t$ to increase and hence the reactive (capacitive) current increases.

The composition of these lipid- or protein-rich domains, although similar, is not uniform and they therefore have different reactive (capacitive) and resistive properties. Their structural similarities produce a collection of similar but not identical relaxation times. When a system possesses a set of similar time constants, rather than generating separate impedance loci for each process, a single locus is produced having a depressed center (8). Therefore, instead of considering the CPE as a collection of transient conducting pathways or "pores", the CPE may be thought of as an ensemble of domains which have closely related time constants.

The magnitude of the reactive (capacitive) current is proportional to the rate of change of potential, $\partial V_m/\partial t$; it is not, therefore, the major component of the membrane current at low frequencies. As the frequency is increased, $\partial V_m/\partial t$ increases, and the reactive (capacitive) current increases. The molecular dipoles present in the lipid/protein-rich domains can orient themselves in response to the changing direction of the field so as to function efficiently as a molecular dielectric, enabling charge to build up at the reactive (capacitive) interface. Thus, at high frequencies, when $\partial V_m/\partial t$ is large, the reactive (capacitive) contribution is the major component of the membrane current.

The response of the phase angle as a function of frequency, for human skin *in vivo*, both in the passive state and after iontophoresis is illustrated in Figure 7a. All the plots exhibit the characteristic increase of the phase angle as the frequency is increased. Iontophoresis produces a change in the variation of the phase angle ($\tan^{-1}\{Z_{Imag}/Z_{Real}\}$) as a function of frequency. The pre-iontophoresis data produce a broad curve, and the initial phase angle is higher, indicating a greater reactive (capacitative) current. In contrast, the slope of the curve is much sharper after iontophoretic current flow. The phase angle after iontophoresis is significantly lower at all frequencies; for example, at 1 Hz (6·3 rad s^{-1}), Δ = 20.8 (where Δ = difference between phase angle prior to and after iontophoresis). In physical terms, this implies that iontophoresis increases the dominance of the resistive pathway as the primary route for current flow, reducing the contribution of the reactive (capacitive) current. It has less

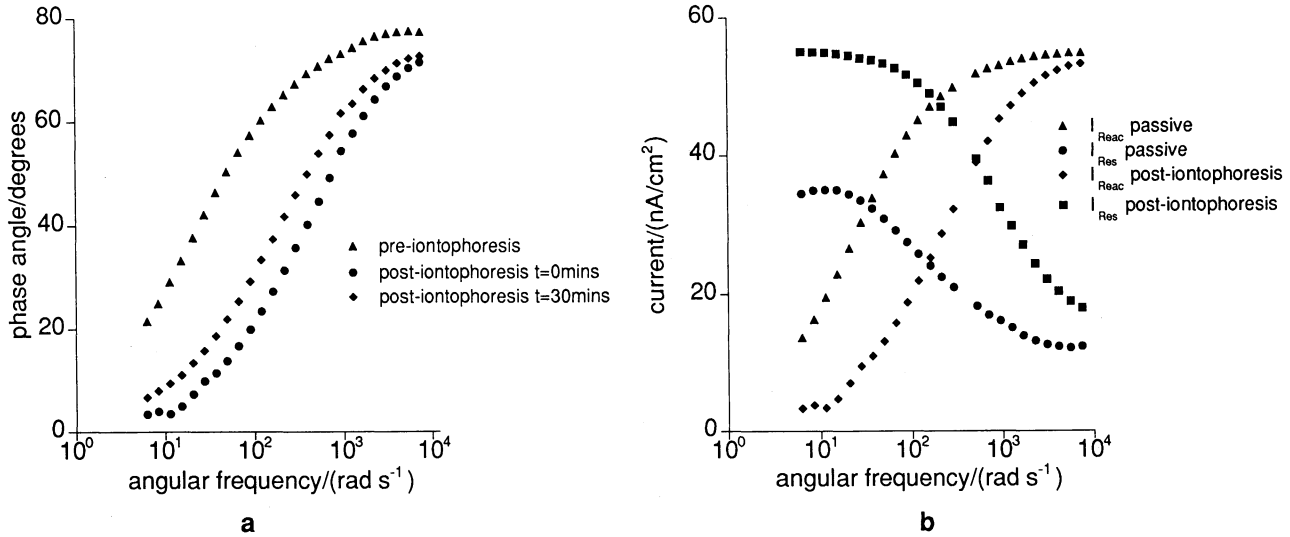

Fig. 7. (a) The variation of the phase angle as a function of frequency before and after iontophoresis. Data from subject B. (b) The resistive and reactive (capacitive) currents as a function of frequency before and after iontophoresis. Data from subject B.

effect at high frequencies as evidenced by the superposition of the plots in this frequency range. The effect of iontophoresis on the resistive and reactive (capacitive) currents is shown in Figure 7b. It is apparent that, after iontophoresis, there is a significant increase in the resistive current component. There is a corresponding decrease in the reactive current over the same frequency range. This latter finding suggests that iontophoresis has its most significant effect on the resistive channels as opposed to the lipid/protein domains, the putative sources of the reactive (capacitive) current.

In conclusion, we have described a comprehensive investigation of the effect of iontophoresis on the impedance properties of human skin *in vivo*. Our data lend support to the idea that ion transport during iontophoresis involves significant participation of the appendageal pathways. Therefore, therapeutic applications of iontophoresis should acknowledge that appreciable current density may flow through this transport pathway when attempting optimization of the technique. We have also shown that impedance spectroscopy can usefully complement transepidermal water loss as a technique for measuring skin permeability *in vivo*.

ACKNOWLEDGMENTS

Supported by the U.S. National Institutes of Health (HD-27839) and by Becton Dickinson. We thank our colleagues in the Skin Bioscience Group, James Uchizono, Lokesh Kalia and Prof. Jon Goerke (UCSF) for their advice, critique and assistance.

REFERENCES

1. P. M. Elias, Epidermal barrier: intracellular lamellar lipid structures, origin, composition and metabolism, *J. Control. Release,* **15**: 199-208 (1991).
2. C. Cullander and R. H. Guy. Transdermal delivery of peptides and proteins. *Adv. Drug Delivery Rev.,* **8**: 291-324 (1992).
3. T. Yamamoto and Y. Yamamoto. Electrical properties of the epidermal stratum corneum. *Med Biol. Eng.* **14**: 151-158 (1976).
4. K. Kontturi, L. Murtomäki, J. Hirvonen, P. Paronen and A. Urtti. Electrochemical characterization of human skin by impedance spectroscopy: the effect of penetration enhancers. *Pharm. Res.* **10**: 381-385 (1993).
5. K. Kontturi and L. Murtomäki. Impedance spectroscopy of human skin. A refined model. *Pharm. Res.,* **11**: 1355-1357 (1994).
6. H. Inada, A. H. Ghanem and W. I. Higuchi. Studies on the effects of applied voltage and duration on human epidermal membrane alteration/recovery and the resultant effects upon iontophoresis. *Pharm. Res.,* **11**: 687-697 (1994).
7. R. R. Burnette. Iontophoresis. In J. Hadgraft and R. H. Guy (eds.), *Drugs and the pharmaceutical sciences* (*Vol. 35*): *Transdermal drug delivery,* Marcel Dekker Inc., New York, 1989, 247-291.
8. J. Z. Bao, C. C. Davis and R. Schmukler. Impedance spectroscopy of human erythrocytes: system calibration and nonlinear modeling. *IEEE Trans. Biomed. Eng.,* **40**: 364-378, (1992).
9. J. R. Macdonald. Impedance spectroscopy. *Ann. Biomed. Eng.,* **20**: 289-305 (1992).
10. J. R. Macdonald. *Complex nonlinear least squares immitance fitting program-LEVM version 6.1,* © Solartron Instruments Ltd., distributed by Scribner Associates, Charlottesville, VA (1994).
11. J. C. Keister and G. B. Kasting. A kinetic model for ion transport across skin. *J. Membr. Sci.,* **71**: 257-271 (1992).
12. R. R. Burnette and B. Ongpipattanakul. Characterization of the pore transport properties and tissue alteration of excised human skin during iontophoresis. *J. Pharm. Sci.,* **77**: 132-137 (1988).
13. C. Cullander and R. H. Guy. Sites of iontophoretic current flow into the skin: identification and characterization with the vibrating probe electrode. *J. Invest. Dermatol.,* **97**: 55-64 (1991).
14. J. J. B. Jack, D. Noble and R. W. Tsien. *Electric current flow in excitable cells*. Oxford University Press, Oxford, (1975).